Materials Chemistry and Physics 226 (2019) 350–355

Contents lists available at ScienceDirect

Materials Chemistry and Physics

journal homepage: www.elsevier.com/locate/matchemphys

Inducing dye-selectivity in graphene oxide for cationic dye separation applications

Pranay Ranjan[a,*], Priyanshu Verma[b], Shweta Agrawal[c], T. Rajagopala Rao[c], Sujoy Kumar Samanta[b,**], Ajay D. Thakur[a,***]

[a] Department of Physics, Indian Institute of Technology Patna, Bihta, 801106, India
[b] Department of Chemical and Biochemical Engineering, Indian Institute of Technology Patna, Bihta, 801106, India
[c] Department of Chemistry, Indian Institute of Technology Patna, Bihta, 801106, India

HIGHLIGHTS

- Elucidate role of excess hydroxyl groups in graphene oxide dye selectivity.
- Density functional theory estimate of adsorption binding energies are estimated.
- Paves way for cationic dye separation.

ARTICLE INFO

Keywords:
Graphene oxide (GO)
Cationic dye adsorption
Selectivity
DFT
Adsorption isotherm

ABSTRACT

Adsorption property of graphene oxide (GO) towards cationic dyes such as methylene blue (MB) and rhodamine B (RhB) has been investigated experimentally. GO structure used in our study is decorated with experimentally observed oxygen functional groups (OFGs). Fast and effective adsorption of MB with GO in single and binary solute solution has been observed experimentally. In support of our experimental data and to understand the interaction of adsorbent (GO) and dye, density functional theory (DFT) calculation has been used for calculating individual binding energy of GO, GO/dye in aqueous medium. Further, study on dye interaction with GO reveals that adsorption was facilitated by presence of oxygen functional group through electrostatic interactions.

Dyes are a major source of water contamination leading to severe health issues [1–10] and a host of techniques [11–13] have been developed in past for the removal of dyes from industrial wastewater. Although inexpensive adsorbents for the removal of dyes exist (see Tables S1–S2), separation of dyes from a dye mixture is a challenging problem. Graphene oxide (GO), a monolayer functionalized sheet of graphene [14–18] is among the most promising material for environmental remediation. It has unique structural property (sp^3 hybridized carbon skeletal) [16–23] and is a amphiphilic material which contains negatively charged functionalities and uncharged aromatic fraction of carbon atoms. These oxygen functionalities are attached to graphene sheets due to chemical or physical interaction of molecule. The interaction of oxygen functionalities (aldehyde, ketonic, alcoholic, epoxide, carboxylic, hydroxyl etc) with graphene leads to covalent bond to the surfaces. Presence of these oxygen functionalities makes the surface charge electro-negative, which leads to adsorption of cationic charge such as methylene blue (MB), methyl orange (MO) etc and repulsion of anionic charge such as rhodamine B (RhB) and acid orange etc. Literature suggests the use of GO in adsorption of cationic dyes from cationic and anionic admixture (see Table S1). However, selecting one cationic dye without adsorbing other dye from a binary mixture of cationic dyes and adsorbing both at a time when required using a suitable adsorbent is a big challenge that needs to be addressed. In this aspect, we synthesized GO [19] and propose a methodology for tuning its functionality for selective adsorption of a cationic dye from a mixture of cationic dyes. To appreciate the effectiveness of GO in dye removal, its adsorption capacity is compared with other adsorbents reported in the literature (see Table S2). We report the selective adsorption of cationic dye from a binary mixture of cationic dyes by exploiting key differences between the gel and foam form of GO

* Corresponding author.
** Corresponding author.
*** Corresponding author.
E-mail addresses: pranjan@iitp.ac.in (P. Ranjan), sksamanta@iitp.ac.in (S.K. Samanta), ajay.thakur@iitp.ac.in (A.D. Thakur).

https://doi.org/10.1016/j.matchemphys.2019.01.047
Received 20 October 2018; Received in revised form 16 January 2019; Accepted 19 January 2019
Available online 23 January 2019
0254-0584/

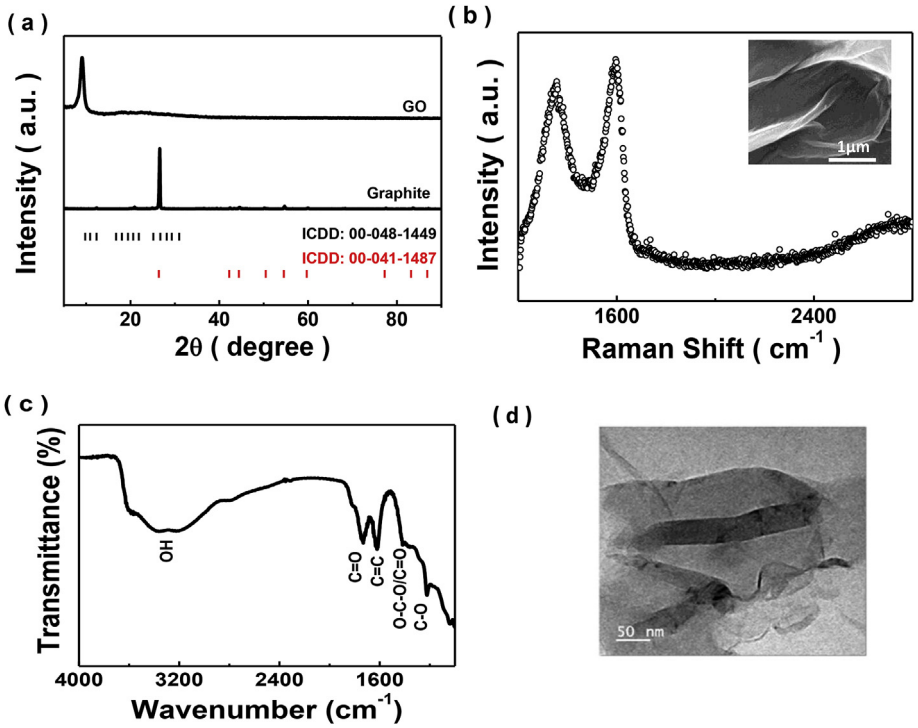

Fig. 1. a) XRD spectrum of GO powder, Graphite and Corresponding ICDD card number (00-048-1449, 00-041-1487), b) Raman spectra of the GO film, inset contains SEM image of GO film, c) FTIR spectra of GO, d) TEM image of GO film.

(described below). The role of –OH functional group in selective adsorption has been investigated making use of density functional theory (DFT).

We made GO using a modified Hummers' method [19] that does not require expensive filtration membranes and is completely non-explosive in nature. Details related to synthesis and characterization tools used for measurement are provided in section 1 of the supplementary information. It was found that the GO gel is obtained after washing of synthesized GO through chemical exfoliation with iso-propyl alcohol, while GO foam was obtained after DI water washing step prior to vacuum drying of GO gel and GO powder is obtained by crushing of GO foam in a mortar and pestle. Here we have used commercially procured GO powder from United Nanotech Innovations Pvt. Ltd. for a comparative study on GO gel, foam and powder (evident from optical image, FTIR spectroscopy and XRD, see SI section 2, Fig. S1). We label this GO gel as GOG. After drying (removal of the alcoholic group by vacuum drying) it becomes GO foam, and therefore we labeled it as GOF. Fig. 1 (a) compares the XRD spectra of GOF and its parent material graphite, while its corresponding ICDD card number has been marked. Diffraction peak at $2\theta = 9.11^{\circ}$ was observed which corresponds to 002 planes of GO [18,19] having an interlayer distance or interlayer spacing of 9.7 Å. The peak observed at 9.11° reveals that oxygen functional groups have been intercalated or introduced in GOF and graphite initial structural skeletal has been destroyed. Further interlayer spacing is also used to know the degree of oxidation, which in our case is good enough to call higher oxygenated GO. XRD spectrum of prepared GOF reveals information about oxidized and non-oxidized graphitic content (which in our case does not exist) as in the 2θ range of 5°–90°, peak at 26° reveals the presence of graphitic domain or non-oxidized graphitic domain. Fig. 1 (b) shows the Raman spectrum of the as-grown GOF film drop-casted on sodium silicate substrate and vacuum dried for an hour. It contains the G band ($1580\,cm^{-1}$) which corresponds to an E_{2g} mode [16–19] and is present due to the vibrational mode of sp^2 bonding of carbon atom, D band ($1350\,cm^{-1}$) [18] or the defect band arises due to imperfection in the hexagonal ring of carbon skeletal. The Raman spectrum of GO contains a hump centered at $2680\,cm^{-1}$ which are attributed to double resonance transition and is an overtone of the D band [17–19]. This occurs due to the addition of functional groups at its basal plane.

Inset of Fig. 1 (b) shows the SEM image of GOF sample drop-casted on a Si/SiO_2 and vacuum dried for an hour. The obtained morphology of GO sheets reveals its layered structure with folds and wrinkles [16–19]. Fig. 1 (c) shows the FTIR spectrum of powder GO sample, which confirms the presence of alcoholic, hydroxyl, ketonic and a carbonyl group. It was found that due to the presence of -OH group [18,19] there is a broadening in the range of $2900–3500\,cm^{-1}$. The peak at $1725\,cm^{-1}$, $1616\,cm^{-1}$ are attributed to carbonyl [19] and –OH group present in GO sample [16–19]. In addition peak at $1224\,cm^{-1}$ and $1055\,cm^{-1}$ are attributed to C-OH group and epoxy group respectively [17]. Fig. 1 (d) shows the TEM image of the GOF sample at length scale of 1 μm. In order to confirm the content of the functional group on the graphitic domain, XPS [19] was used to measure sp^3 content in our GO sample and it was found to be 59.4%. To distinguish the change between GO gel, GO foam and GO powder (see SI section 2 and Fig. S1). After confirmation of phase purity, we fixed the dye concentration as 10 ppm and amount of GOG, GOF as 280 ppm. To begin with, we added an equal amount of GO-G (100 parts per million, ppm) in all the four dyes (with concentration of 10 ppm each) and kept it under observation. We found that after 5 min there is the appearance of black color sludge in GO-G mixed with MB. To make sure that GO-G synthesized by our technique does not affect the other three dyes, we waited to observe for next 24 h and found no visual change in color of dye as well as the formation of sludge. Overall in this experiment, we found that only MB has shown effective adsorption in presence of GO-G (see Fig. 2(a)), as flocs of MB-GO-G can be easily visualized. Therefore, MB has been considered for further studies in this work.

A dose optimization experiment has also been performed for the effective removal of MB from the water. For the same, different known GO-G concentrations (10, 50, 100, 200, 300, 400 and 500 ppm) have been used for removal of 10 ppm of MB dye in a fixed time duration (i.e., 10 min). The obtained results have been shown in Fig. 2 (b) (visual

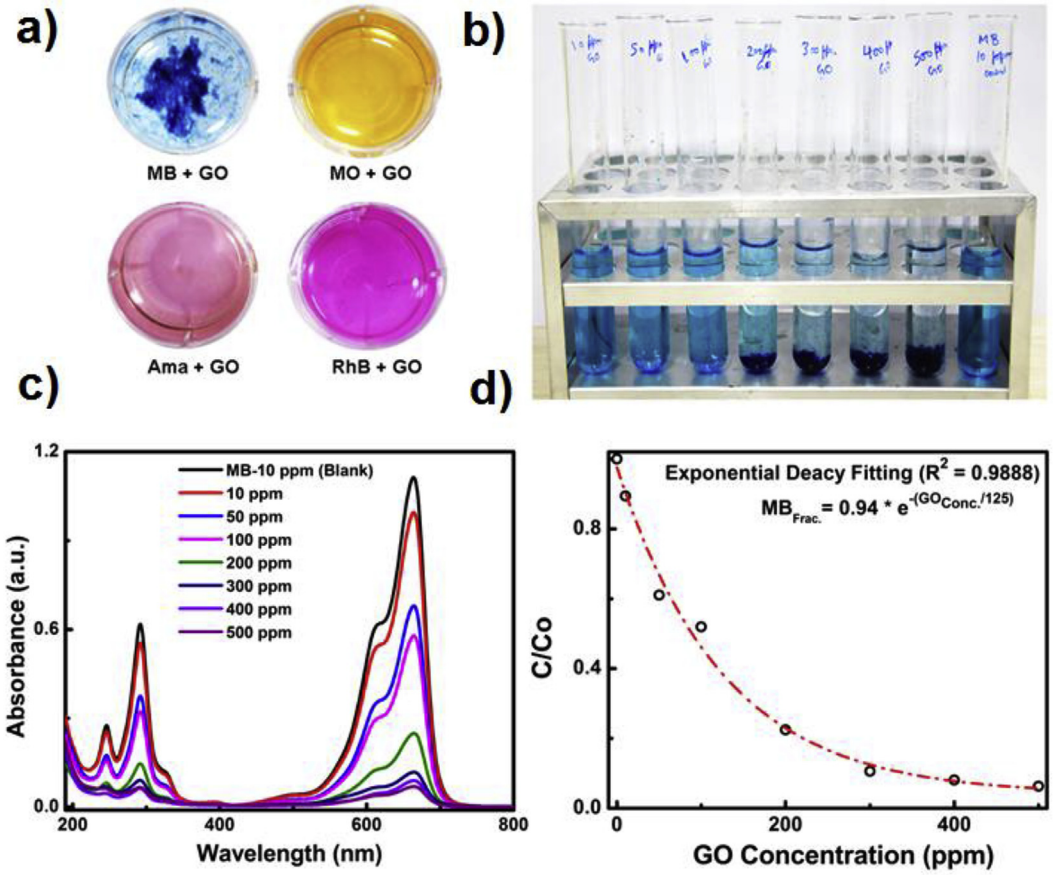

Fig. 2. a) Visual image of different dye in water along with GO-G, b) Different concentration of GO-G in 10 ppm MB solution in water, c) UV–Vis spectrum of MB with different GO-G concentration in water, d) Exponential curve fitting of GO-G adsorption on MB at different ppm.

observation). Correspondingly, its UV–Visible spectrum is obtained and has been plotted in Fig. 2 (c). It has also been fitted with an exponential decay (Fig. 2 (d)) curve with better regression coefficient value ($r^2 = 0.9888$). The optimum dose of GO-G for 90% removal of MB has been calculated with the obtained mathematical relation that has given a value of about 280 ppm GO-G for 10 ppm MB dye. However, increase in GO-G concentration has shown no further improvement in the results, hence have been neglected to make a trade-off between the amounts of GO-G used.

To observe the difference in adsorption property of GOG and GOF; we did a comparative adsorption study on GOG, GOF on individual and mixed dyes (see Fig. 3). To our delight, we found that GOG is able to degrade MB but not RhB (see Fig. 3(b) and (d)). Interestingly, GOF is able to degrade both the individual dyes (see Fig. 3 (a) and (c)). Having glimpse regarding the selective adsorption of GOG, natural curiosity is whether GOG is able to separate MB out of the binary mixture (MB + RhB) of dyes or not. To our surprise, we found that GOG can selectively remove MB in a binary mixture of dyes (see Fig. 3 (e)). In contrast to this GOF was found to adsorb both the dyes (see Fig. 3 (e)). The camera image of experimental observation is shown in Fig. 3 (f)). Appreciably more amount of functional group in GOG as compared to GOF has been a huge encouragement. To differentiate the quantitative analysis of functional group (which leads to selective adsorption) in GOG and GOF we compared the FTIR spectra of the two samples (see Fig. 4).

It was observed that GOG contains more number of –OH group than GOF (one of the most feasible conditions for dye selectivity in DFT, discussed later) as shown in Fig. 4. Monolayer sheet of GO structure (7 X 7 carbon atom ring) containing oxygen functionalities such as carboxylic, ketonic, ether, and alcoholic groups was optimized using Gaussian16 (see Fig. S3) [24–29] by Minnesota functional M06-2X [28] and 6-31G basis set [29]. The optimized molecular formula of GO sheet used for calculation is $C_{132}H_{25}O_{31}$ with C:O ratio being 4.25:1 [30]. The oxygen functionalities were randomly distributed on the surface of graphene oxide, and the edges were passivated by hydrogen atoms. Since, GO contains oxygen functionalities and has an electronegative charged surface, therefore to study the interaction of GO with different dyes we have chosen cationic dyes (MB, RhB) only. To calculate the binding energy of GO with dye, the dye molecules are added in parallel to the GO sheet and were optimized (see Fig. S4). Both RhB and MB were placed in parallel orientation to GO and the complexes were re-iterated for energy minimization in gaseous as well as aqueous phase. Fig. S4 shows the optimized structure of GO and dyes when kept in close proximity in gaseous and aqueous phase. It was found that both the dye molecules show an affinity towards adsorption when placed parallel to the optimized geometry of GO. The binding energy between the dye and GO is calculated using the relation [30].

$$E_b = E_{(dye+GO)} - (E_{(dye)} + E_{(GO)})$$

where, E_b is the binding energy, $E_{(dye+GO)}$ is the total energy of the dye adsorbed on GO, $E_{(dye)}$ is the total energy of the dye molecule and $E_{(GO)}$ is the total energy of the monolayer GO surface. While the bandgap or energy gap is calculated using relation:

$$E_g = E_{HOMO} - E_{LUMO}$$

where, E_g is the difference between HOMO and LUMO molecular orbital level. E_{HOMO} is defined as the energy of the highest occupied energy level, E_{LUMO} as the energy of the lowest occupied molecular energy level. The calculated HOMO values for GO + MB, GO + RhB in gas phase using M06-2X is −0.20729, −0.20784 Hartree and in aqueous

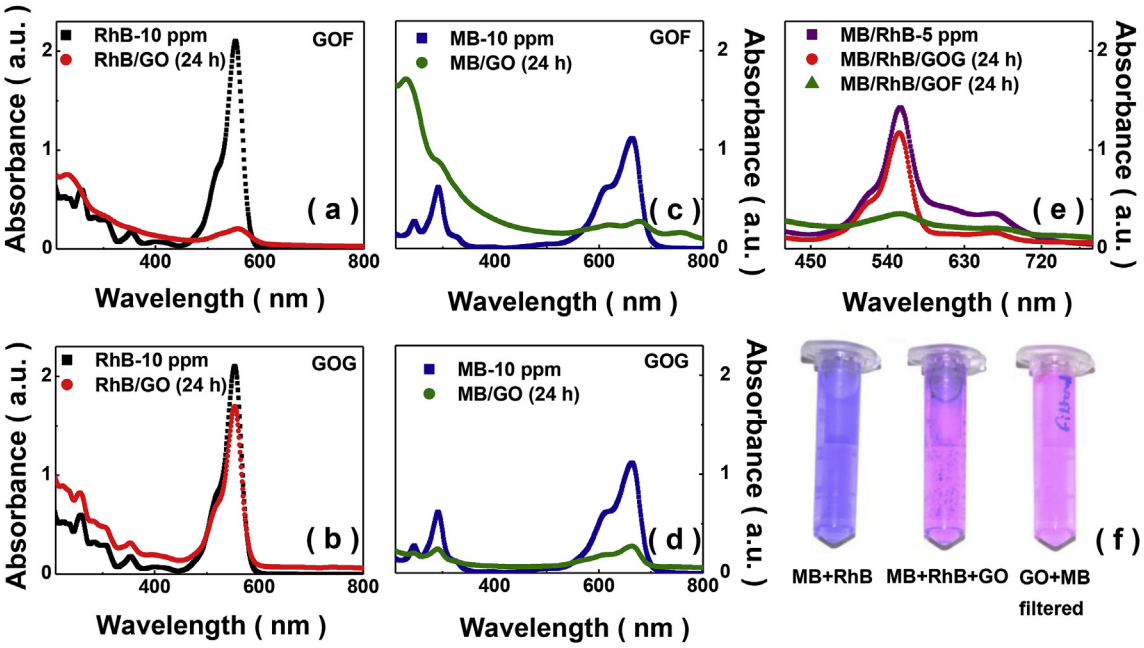

Fig. 3. UV–Visible adsorption spectra of GOF onto RhB, MB dye in (a), (b). Using GOG in (c), (d), (e) UV–Visible absorption of GOG, GOF onto binary mixture MB/RhB dyes respectively and (f) Optical image of the tube containing MB/RhB, MB/RhB/GO and RhB (GO-MB filtered).

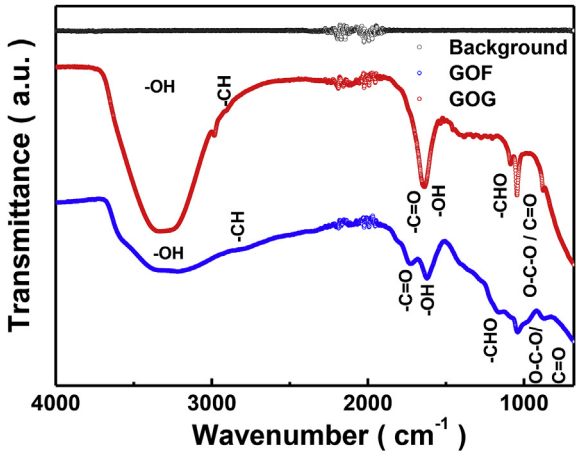

Fig. 4. FTIR spectrum of GOG and GOF. A background spectrum has also been plotted.

phase it is −0.20798, −0.20519 Hartree respectively. Moreover, calculated LUMO values using M06-2X for GO + MB and GO + RhB in gas phase are −0.17142, −0.16526 Hartree and in aqueous phase it is −0.16026, −0.16019 Hartree respectively. The band gap, therefore calculated from above equation gives a value of −0.03587, −0.04772 Hartree for GO + MB in gas and aqueous phase, while for GO + RhB it is −0.04258 and −0.0450 Hartree in gas and aqueous phase.

A binding energy for GOG/MB structure is calculated as −0.21 ± 0.02 Hartree and −0.15 ± 0.01 Hartree in gas and aqueous phase, respectively. While for GOG/RhB, it is −0.08 ± 0.02 Hartree and −0.07 ± 0.02 Hartree for gas and aqueous phase, respectively. In order to see the convergence of our result using basis set 6-31G in our study, we also performed DFT using higher basis set 6-31G(d,p) for GOG/MB and GOG/RhB in aqueous phase. We obtained a binding energy of −0.22 Hartree and −0.10 Hartree for GOG/MB and GOG/RhB in aqueous phase. This indicates a condition when both the dyes (MB, RhB) if present simultaneously can be adsorb by GO. However, our goal is to realize the structure of GO for selective adsorption of cationic dyes (GOG), therefore we made a GO structure which can make GO/RhB binding energy positive (repulsion) and to that of GO/MB in the negative (attractive). It is easy to tune the amount of one functional group attached to graphene oxide structure theoretically but practically this job is impossible. Therefore, we considered a more favorable case which is theoretically as well as practically possible. We tuned the ratio of the only alcoholic group (-OH group) in graphene oxide and studied its interaction with MB and RhB. Experimentally this job can be made feasible by adding ethanol or iso-propyl alcohol to GO, thus making GOG. To realize our goal, we made GOG structures with a different number of –OH group (GOG-1). We made three cases in which a different number of –OH group in GOG structure has been added i.e from three, seven to nine while the number of other functional group remains constant in all the cases. The fraction of –OH group is calculated by calculating a number of –OH group attached to GO divided by a number of active sites (in our case 128 carbon atom) in GO sheet, without considering other functionalities carbon atom.

A plot of binding energy (GOG-1/RhB and GOG-2/RhB) as a function of a number of –OH functional group is shown in Fig. 5 (a), (b). To our surprise, we found that as the number of –OH group is increasing a repulsive force is acting between GOG-1/RhB. Side view optimized structure of GOG-1/RhB and GOG-2/RhB is shown in see Fig. 5 (c), (d), (e) and Fig. 5 (f), (g), (h) respectively. In order to further substantiate our result and to eliminate any confusion of obtaining positive (repulsive) energy between GOG-1/RhB, we made another structure of GOG (GOG-2) with different number (two, seven and eleven) of –OH group and optimized the structure (GO/RhB) in aqueous phase (see Fig. 5 (f), (g) and (h)). The result (see Fig. 5) is again surprising as we found that increasing –OH group make GOG surface repulsive to RhB. Hence from Fig. 5 (a), (b) it can be infer that as the amount of –OH group is decreased the binding gets increased (electrostatic attraction) for RhB dye towards GOG, and as the fraction of –OH gets increased binding energy turnout to be positive (electrostatic repulsion) which signify repulsion for RhB dye. DFT binding energy calculation thus supports our experimental findings.

After optimization of GOG with MB and RHB dyes we calculated adsorbent-adsorbate systems as follows; MB is found to be chemisorbed on the GO surface by attaching with –OH group at the surface of GO and having an interaction distance of 1.95 Å. While the inter-atomic distance between nitrogen atoms to an oxygen atom in carbonyl group is

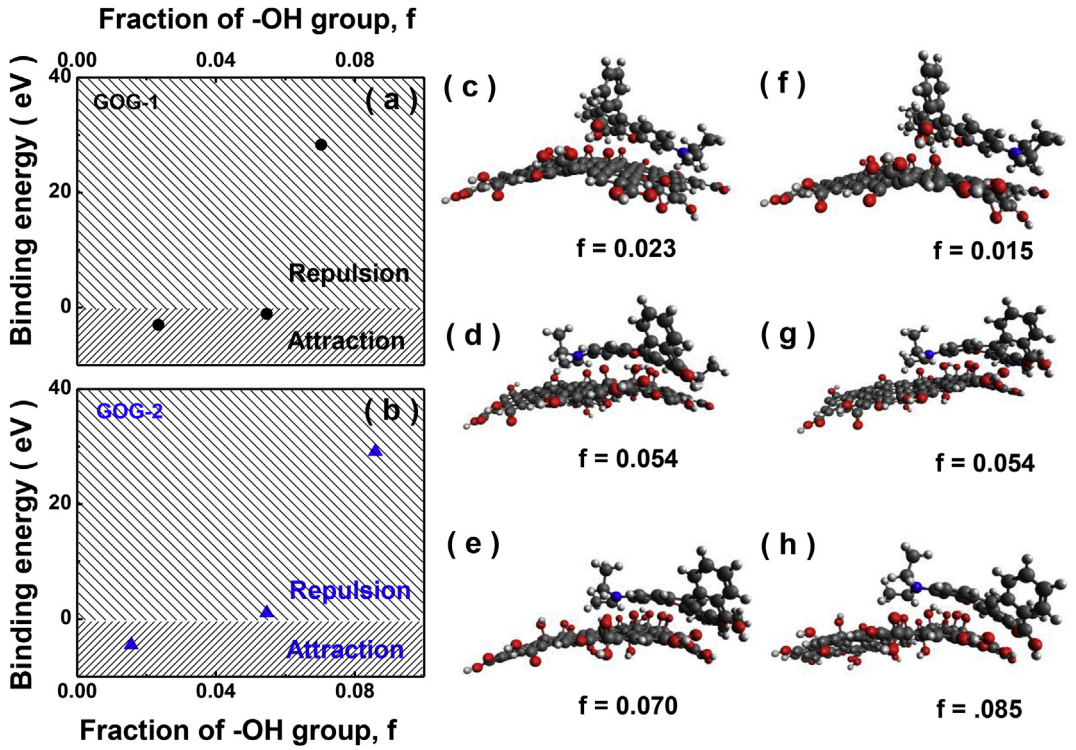

Fig. 5. Binding energy vs. the fraction of –OH group of a) GOG-1/RhB, b) GOG-2/RhB obtained from GOG/RhB interaction. Side view optimized geometry of GOG-1/RhB ((c), (d), (e)) and GOG-2/RhB ((f), (g), (h)) containing different fraction of –OH group.

found to be 1.75 Å. The electronegative atom S tends to attract an epoxy group with an inter-atomic distance of 5.46 Å, exhibiting a non-covalent interaction towards GO.

Similarly, RhB shows attraction towards functional group between the nitrogen atom and oxygen present of carbonyl group with an inter-atomic distance of 3.36 Å. While the distance between a hydrogen atom and an oxygen atom in the carboxylic group is found to be 1.14 Å. We infer that among both dye molecules, the binding energy of GO/MB is found to be more than GO/RhB indicating a high chance of MB adsorption to the surface of GO.

We have also employed DFT for calculating thermodynamic parameters at room temperature (T = 298.15 K). The enthalpy of GOG/MB in gas phase and aqueous phase was 35.75, 13.16 K cal/mol and for GOG/RhB in gas and aqueous phases was −34.90, −52.42 K cal/mol. The free energy calculation for GOG + MB in gas and aqueous phase was 50.17, 27.13, K cal/mol and for GOG/RhB in gas and aqueous phase was −47.88, −39.88 K cal/mol respectively.

The Minnesota, M06 family of functions seem to be a good choice for handling molecular system where weak intermolecular interactions such as non-covalent interactions exist [35]. The parameters of the M062X functions are optimized to minimize the errors associated with a number of molecular properties and not just non-covalent interaction [30]. M062X functional is able to approximate model dispersion interaction [35]. There are other methods including dispersion correction such as GD3 correction (for B3LYP) which may contribute significant improvement in accuracy therefore here we compare our previous result with this dispersion corrected B3LYPD3 method. We calculated binding energy for RhB with graphene oxide with 7 and 9 -OH functional group. A binding energy of −3.8 Hartree was found using B3LYPD3 and correspondingly −0.07 Hartree using M062X is calculated for GOG-1 with 7 -OH group. Moreover, for 9 –OH group we found −1.6 Hartree using B3LYPD3 and correspondingly +1.794 using M062X for GOG-1 with 9 -OH group in aqueous phase. This present data with previous calculation is varying quantitatively but qualitatively the binding energy is decreasing with increase of -OH group.

To find the possible ways why GOG responded only to MB even though MB [31,32] and RhB [33,34] both are cationic dyes, we move on to detailed experimental. A selectivity test has been performed to show and confirm the selective removal of MB dye over MB + RhB mixture (see Fig. 6 (a)). It should be noted that GOG is not degrading MB dye molecules. To understand the method of adsorption we have calculated the kinetic model of adsorption of mixture of dye (MB + RhB) on GO (see Table 1). It is basically acting as a flocculating agent that causes the formation of GOG-MB (graphene oxide-gel-methylene blue) flocs. These GOG-MB flocs have a tendency to settle down slowly under the influence of gravity. However, it can also be speed-up with the help of additional centrifugal forces. In that way, we can transfer pollutants from aqueous matrix to solid form, where they can be easily separated or treated out. Besides this, a slighter decrement in RhB concentration is also observed that was probably due to the GOG-MB flocs mediated removal of RhB, which is quite insignificant. It was found that there is an increment of RhB intensity (peak at 554 nm) after addition of GOG solution (see Fig. 6 (b)). However, there is a decrement in peak intensity of MB (peak at 664 nm) which might be attributed to the formation of flocs. It took 3 min by UV–Vis spectrophotometer to acquire a full scan of dye spectra for a single sample. Computational details, and details of the dye sensing mechanism to GOG and adsorption isotherm are discussed in SI section 3.1 to 3.4. Fig. 6 shows the experimental observation of selective removal of MB dye from MB + RhB mixture. It was found that GOG adsorbs MB within 5 min, while RhB does not get adsorbed over 24 h.

To conclude, we successfully demonstrated (experimentally) the separation of a cationic dye RhB from a binary mixture of cationic dyes (RhB and MB) using GO. The optimal dose of GOG for adsorption of MB was obtained through a series of the UV–Visible absorption experiment. The structural difference between GOG and GOF was uncovered using FTIR. DFT was employed for optimizing the structure of GO with a different fraction of –OH group and dyes. The electrostatic energy between adsorbate and dyes reveals a binding energy of −0.15 Hartree for GOG/MB and −0.07 Hartree for GOG/RhB in aqueous phase.

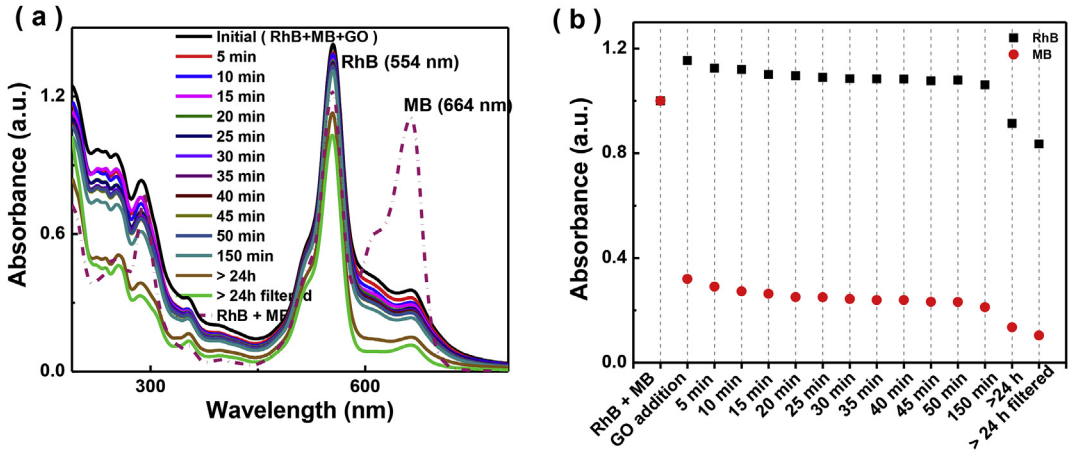

Fig. 6. a) UV–Vis spectrum of RhB/MB/GOG obtained at different times and b) experimental realization of selectivity based on a comparison of MB and RhB adsorption using UV–Vis spectroscopy.

Table 1
Kinetic parameter for MB + RhB dye adsorption onto GO at 298K.

Kinetics		RhB	MB
Pseudo-first order	q_e(mg/g)	6.3	28.79
	k_1 (min^{-1})	0.0068	0.0598
	R^2	0.83303	0.75485
Pseudo-second order	q_e (mg/g)	2.81	25.90
	k_2 ($g.mg^{-1}.min^{-1}$)	0.0257	0.0544
	R^2	0.97846	0.99991

Moreover, tuning of –OH group leads to a variation of binding energy from −4.48 eV to 29.11 eV. This behaviour of dye adsorption in a single and binary solution of cationic dyes makes GO an ideal candidate for environmental remediation and provides scope for recovery of valuable dyes. This is expected to invigorate further work on inducing selectivity in dye adsorption property in GO as is expected to widen the scope for its applications in dye adsorption and water purification.

Funding

The authors thank Ministry of Human Resources Development, MHRD (India) for financial support.

Appendix A. Supplementary data

Supplementary data to this article can be found online at https://doi.org/10.1016/j.matchemphys.2019.01.047.

References

[1] P. Verma, S. Kumar, Environ. Chem. Lett. 16 (2018) 969–1007.
[2] Y.C. Sharma, Uma, J. Chem. Eng. Data 55 (2010) 435–439.
[3] Y.C. Sharma, Uma, A.S.K. Sinha, et al., J. Chem. Eng. Data 55 (2010) 2662–2667.
[4] M.T. Yagub, T.K. Sen, S. Afroze, et al., Adv. Colloid Interface Sci. 209 (2014) 172–184.
[5] P. Verma, S. Kumar, Res. Chem. Intermed. 44 (2017) 1963–1988.
[6] P. Verma, S. Kumar, Res. Chem. Intermed. 43 (2017) 6317–6341.
[7] M.M. Ayad, A.A. El-Nasr, J. Phys. Chem. C 114 (2010) 14377–14383.
[8] X. Wang, Y. Liu, H. Pang, S. Yu, Y. Ai, X. Ma, G. Song, T. Hayat, A. Alsaedi, X. Wang, Chem. Eng. J. 344 (2018) 380–390.
[9] S. Yu, X. Wang, W. Yao, J. Wang, Y. Ji, Y. Ai, A. Alsaedi, T. Hayat, X. Wang, Environ. Sci. Technol. 51 (2017) 3278–3286.
[10] S. Yu, X. Wang, Y. Ai, X. Tan, T. Hayat, W. Hu, X. Wang, J. Mater. Chem. A 4 (2016) 5654–5662.
[11] R.J. Stephenson, S.J.B. Duff, Water Res. 30 (1996) 781–792.
[12] M.S. Chiou, G.S. Chuang, Chemosphere 62 (2006) 731–740.
[13] V.K. Gupta, S. Khamparia, I. Tyagi, et al., J. Environ. Sci. Manag. 1 (2015) 71–94.
[14] W.S. Hummers, R.E. Offeman, J. Am. Chem. Soc. 80 (1958) 1339.
[15] B.C. Brodie, Phil. Trans. Roy. Soc. Lond. 149 (1859) 249–259.
[16] M. Hirata, T. Gotou, S. Horiuchi, et al., Carbon 42 (2004) 2929–2937.
[17] N.I. Kovtyukhova, Chem. Mater. 11 (1999) 771–778.
[18] D.C. Marcano, D.V. Kosynkin, J.M. Berlin, et al., ACS Nano 4 (2010) 4806–4814.
[19] P. Ranjan, Shweta, A. Sinha, T.R. Rao, J. Balakrishnan, A.D. Thakur, Sci. Rep. 8 (2018) 12007.
[20] J. Lu, Y. Li, S. Li, S.P. Jiang, Sci. Rep. 6 (2016) 21530.
[21] C. Liu, F. Hao, X. Zhao, Q. Zhao, S. Luo, H. Lin, Sci. Rep. 4 (2014) 3965.
[22] C. Sarkar, S.K. Dolui, RSC Adv. 5 (2015) 60763.
[23] S. Eigler, S. Grimm, F. Hof, A. Hirsh, J. Mater. Chem. A. 1 (2013) 11559.
[24] H. Bai, W. Jiang, G.P. Kotchey, W.A. Saidi, B.J. Bythell, J.M. Jarvis, A.G. Marshall, R.A.S. Robinson, A. Star, J. Phys. Chem. C 118 (2014) 10519–10529.
[25] K. Song, Y. Long, X. Wang, G. Zhou, Nano Res. 11 (2018) 254–263.
[26] M. Lundie, Z. Sljivancanin, S. Tomic, J. Mater. Chem. C. 3 (2015) 7632–7641.
[27] K.Z. Kamali, A. Pandikumar, G. Sivaraman, H.N. Lim, S.P. Wren, T. Sun, N.M. Huang, RSC Adv. 5 (2015) 17809–17816.
[28] Y. Zhao, D.G. Truhlar, Theor. Chem. Acc. 120 (2008) 215–241.
[29] V.A. Rassolov, M.A. Ratner, J.A. Pople, et al., J. Comput. Chem. 22 (2001) 976–984.
[30] C.R. Minitha, M. Lalitha, Y.L. Jeyachandran, et al., Mater. Chem. Phys. 194 (2017) 243–252.
[31] M. Zhao, P. Liu, Desalination 249 (2009) 331–336.
[32] S.T. Yang, S. Chen, Y. Chang, A. Cao, Y. Liu, H. Wang, J. Colloid Interface Sci. 359 (2011) 24–29.
[33] J. Zhao, W. Ren, H.M. Cheng, J. Mater. Chem. 22 (2012) 20197.
[34] Z. Sui, Q. Meng, X. Zhang, R. Ma, B. Cao, J. Mater. Chem. 22 (2012) 8767.
[35] M. Walker, A.J. Harvey, A. Sen, C.E. Dessent, J. Phys. Chem. 117 (2013) 12590–12600.